

Tracing the imprints of large-scale magnetized structure on γ rays from GRB 221009A

Saikat Das,^{a,b} Soebur Razzaque,^{c,d,e} Nestor Mirabal,^{f,g,h} Nicola Omodei,ⁱ Kohta Murase,^{j,a} Israel Martinez-Castellanos^k

^aCenter for Gravitational Physics and Quantum Information, Yukawa Institute for Theoretical Physics, Kyoto University, Kyoto 606-8502, Japan

^bDepartment of Physics, University of Florida, Gainesville, FL 32611, USA

^cCentre for Astro-Particle Physics (CAPP) and Department of Physics, University of Johannesburg, PO Box 524, Auckland Park 2006, South Africa

^dDepartment of Physics, The George Washington University, Washington, DC 20052, USA

^eNational Institute for Theoretical and Computational Sciences (NITheCS), Private Bag X1, Matieland, South Africa

^fCenter for Space Sciences and Technology, University of Maryland, Baltimore County, Baltimore, MD 21250

^gMail Code 661, Astroparticle Physics Laboratory, NASA Goddard Space Flight Center, Greenbelt, MD 20771, USA

^hCenter for Research and Exploration in Space Science and Technology, NASA Goddard Space Flight Center, Greenbelt, MD 20771

ⁱW. W. Hansen Experimental Physics Laboratory, Kavli Institute for Particle Astrophysics and Cosmology, Department of Physics and SLAC National Accelerator Laboratory, Stanford University, Stanford, CA 94305, USA

^jDepartment of Physics; Department of Astronomy & Astrophysics; Center for Multimessenger Astrophysics, Institute for Gravitation and the Cosmos, The Pennsylvania State University, University Park, PA 16802, USA

^kDept. of Physics, University of Maryland, College Park, MD 20742, USA

E-mail: saikatdas@ufl.edu, srazzaque@uj.ac.za, nestor.r.mirabalbarrios@nasa.gov

Abstract. We search for possible GeV-TeV gamma-ray imprints of ultrahigh-energy (UHE; $\gtrsim 0.1$ EeV) cosmic ray (CR) acceleration in the large-scale structures surrounding the brightest gamma-ray burst (GRB) explosion, GRB 221009A. Using 1.25 years of post-event *Fermi* Large Area Telescope (LAT) data, we construct a 1 GeV – 1 TeV test-statistic (TS) map within 15 Mpc of the burst. We identify two peaks in the TS map with $TS \geq 9$. The most significant peak, J1911.8+2044, exhibits gamma-ray emission in pre-burst LAT data. The other peak, J1913.2+1901, coincides with a 664.6 GeV photon recorded ~ 191.9 days after the GRB trigger and located at about 0.75° from the GRB localization. The per-photon 95% containment angle for the LAT is about 0.25° in the 100 GeV – 1 TeV energy range. We explore two possible origins for the γ -ray emission: (1) UHECRs from GRB 221009A propagating through a magnetized cosmological volume in its vicinity, and (2) UHE or very-high-energy (VHE; $\gtrsim 100$ GeV) γ -ray emission from GRB 221009A, propagating in the same volume. In both cases, electromagnetic cascade emission is induced in the structured region embedding the burst. If any TS features are related to large-scale imprints induced by cosmic rays, it might be further evidence that GRB 221009A accelerated UHECRs. However, our results show that alternative scenarios without invoking UHECRs cannot be ruled out, and the observed high-energy photon could be unrelated to GRB 221009A.

Contents

1	Introduction	1
2	<i>Fermi</i>-LAT analysis	3
3	Potential Explanations	5
3.1	UHE proton-induced cascade emission	6
3.1.1	Simulation setup	7
3.1.2	Propagation in structured regions	8
3.1.3	Propagation in void regions	9
3.1.4	Broadband spectrum and energy requirement	10
3.2	UHE/VHE γ -ray-induced cascade emission	11
4	Calculation of the expected number of events	13
5	Summary and Conclusions	13

1 Introduction

GRB 221009A is the most luminous gamma-ray burst (GRB) recorded in more than 50 years of γ -ray observations [1]. Complete afterglow emission was observed for the first time from a GRB, due to the source being within the field of view of the Large High Altitude Air Shower Observatory (LHAASO) [2, 3]. High-energy photons with energy up to 13 TeV have been detected by LHAASO, with more than 140 γ -ray photons detected above 3 TeV. These photons arrived within 230-900 s after the *Fermi* Gamma-Ray Burst Monitor (GBM) was triggered on 9 October 2022, at 13:16:59.99 Universal Time (T_0) [4]. *Fermi*-GBM has observed two distinct emission characteristics. An isolated emission peak between T_0 and $T_0 + 20$ s was observed by GBM and other γ -ray detectors, corresponding to a highly variable emission in the MeV energy range. An extended emission over $T_0 + 220$ s to $T_0 + 550$ s corresponds to the VHE ($\varepsilon_\gamma \gtrsim 100$ GeV) γ -ray flux, having a smooth temporal profile. *Fermi* Large Area Telescope (*Fermi*-LAT) detected the highest energy γ -ray photon of energy 99.3 GeV from this GRB, 240 s after the trigger [5–7]. In addition, *Fermi*-LAT has recently reported the detection of a 400 GeV photon, 33 ks after the trigger, which is incompatible with a pure leptonic or associated TeV electromagnetic cascade emission [8], indicating a possible hadronic origin.

The unusual characteristics of this GRB event and the broad coverage over a wide range of energies, from radio to VHE γ rays, have offered critical insight into GRB physics and the origin of high-energy cosmic rays, γ rays, and neutrinos [9]. Recent studies on GRB 221009A have proposed that $\gtrsim 10$ TeV γ rays detected by LHAASO can be attributed to the secondary emission from ultrahigh-energy (UHE; $\varepsilon \gtrsim 0.1$ EeV) cosmic rays (CRs) injected by the GRB in the intergalactic medium [10–12]. Motivated by the *Fermi*-LAT detection of a VHE photon (~ 664.6 GeV) appearing 191.9 days after the *Fermi*-GBM trigger, at an angular offset of 0.75° from the GRB’s direction, we investigate the possibility of UHECR-induced emission within the large-scale magnetized structures surrounding a GRB [13]. In addition, we explore the possible origin of this photon in the electromagnetic cascade flux at Earth resulting

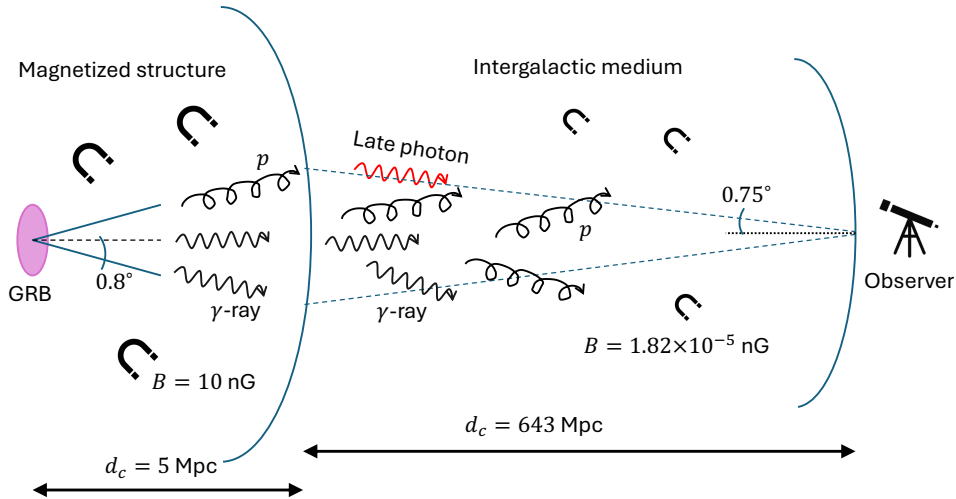


Figure 1. Schematic representation showing the two distinct regions, viz., the magnetized structure in which the GRB is embedded and the void region. We consider a comoving distance scale of $d_c \sim 5$ Mpc for the structured region. The void intergalactic medium with a much weaker magnetic field extends for $d_c \sim 643$ Mpc.

from the emission of UHE or VHE γ rays. This analysis is also crucial to understanding the propagation of cosmic rays in magnetized cosmological volumes and the associated time delays in observed photon signals. Large-scale structures can correspond to galaxy clusters, filaments, or magnetic voids surrounding the GRB 221009A host galaxy. In particular, recent studies show from fitting LHAASO data that voids likely surround GRB 221009A, see [12, 14].

We analyze 1 GeV–1 TeV data from *Fermi*-LAT starting 5.73 days after the burst (once the initial GRB γ -ray emission has subsided [7]) and extending to 456.69 days after the burst. We show a schematic representation of our model considerations in Figure 1. Here, we have two zones, viz., the host galaxy of the GRB is embedded in a large-scale magnetized structure with a high magnetic field intensity. The UHECRs and γ rays injected by the GRB jet propagate in this medium and subsequently through the intergalactic medium before reaching the observer. We consider two plausible scenarios to explain the origin of delayed γ rays from this GRB. In the first scenario, the UHECRs injected by the GRB jet initiate an electromagnetic cascade, producing secondary TeV photons. The UHECRs experience significant deflection in the highly magnetized structured region surrounding the burst, leading to delayed arrival of photons at the position of the observer. Thus, the late photon originates from the flux emerging from the large-scale structure in an annular region at a semi-apex angle comparable to the angular offset of $\sim 0.75^\circ$. The secondary UHECRs from the structured region undergo further deflection in the extragalactic medium and initiate an electromagnetic cascade, resulting in a cosmogenic γ -ray spectrum.

In the second scenario, the unattenuated synchrotron self-Compton (SSC) emission from the GRB jet cascades to GeV–TeV energies. In this case, photons only suffer additional energy loss during propagation over the intergalactic medium. However, the observed late photon signal originates from deflected photons emerging from this structured region, which can be primarily due to the jet opening angle and also the deflection of secondary electrons. We compare the energy budget required for UHE proton-induced cascades and UHE γ -ray-induced emission with the total energy released in the GRB blastwave. Our findings suggest

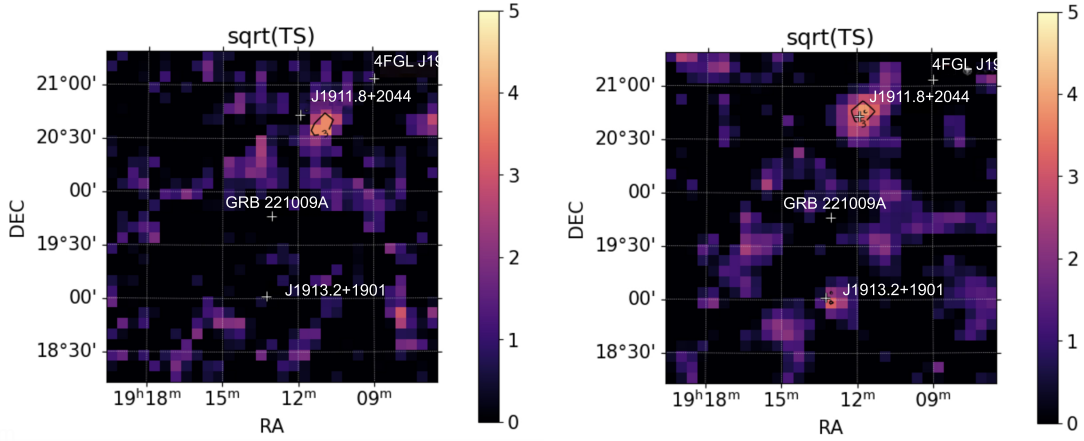


Figure 2. Left panel: TS map (1 GeV – 1 TeV) of the $3^\circ \times 3^\circ$ region centered on GRB 221009A using 14.2 years of pre-burst *Fermi*-LAT data. Right panel: TS map generated using LAT data from 5.73 to 456.69 days after the GBM trigger for GRB 221009A. In both cases, J1911.8+2044 and J1913.2+1901 are excluded from the model. The white cross in the center of the figure marks the location of GRB 221009A.

that both scenarios are viable, though further statistical improvements will provide definitive tests. In both cases, we assume that the delay induced by the intergalactic medium, which lies between the structured region and the observer, is sub-dominant compared to the structured region.

The paper is organized as follows. In Sec. 2, we present the *Fermi*-LAT analysis of the GeV-TeV emission from the GRB. Sec. 3 presents the plausible explanations of the late photon observation from this GRB by *Fermi*-LAT. We calculate the expected number of events and check the consistency with the theoretical model in Sec. 4. We discuss our results and implications in Sec. 5. Throughout the paper, we assume a Flat Λ CDM cosmology with $H_0 = 69.6 \text{ km s}^{-1} \text{ Mpc}^{-1}$, $\Omega_m = 0.286$, and $\Omega_\Lambda = 0.714$.

2 *Fermi*-LAT analysis

To study large-scale γ -ray emission in the region around the GRB 221009A event, we used the *Fermitools* package (v.2.2.0) and *fermipy* package (v.1.2.0) to produce a test-statistic (TS) map of the GRB 221009A region. The TS map covers a region of interest (ROI) of $10^\circ \times 10^\circ$ area with pixel size of 0.1° . A TS map is generated by adding a tentative point source at each location and then calculating the likelihood ratio between the previously optimized model and the best-fit model with the additional source at that location. Here, the test statistic is defined as $\text{TS} = -2 \log \left(\frac{\mathcal{L}_0}{\mathcal{L}_s} \right)$, where \mathcal{L}_0 is the likelihood of the original model and \mathcal{L}_s is the likelihood of the model with the additional source. To avoid contamination from the GRB, we used 1 GeV–1 TeV events from 5.73 to 456.69 days after the burst trigger [7]. We selected P8R3_SOURCE_V3 events with event class `evclass = 128/ FRONT+BACK` event types (`evtype=3`) and maximum zenith angle cut at 90° to minimize Earth limb contamination. Additional contributions from nearby point sources were modeled using the 4FGL-DR3 catalog and standard background templates for the Galactic diffuse emission (`gll_iem_v07.fits`) and the isotropic component (`iso_P8R3_SOURCE_V3_v1.txt`) within 15° of the ROI center.

Table 1. Sources Detected with $TS > 9$

Designation	RA degrees	Dec. degrees	TS	95% Flux UL (1 GeV–1 TeV) $\text{erg cm}^2 \text{s}^{-1}$
J1911.8+2044	287.979 ± 0.070	20.720 ± 0.070	17.9	7.0×10^{-12}
J1913.2+1901	288.307 ± 0.120	19.011 ± 0.120	10.6	4.3×10^{-12}

We generated TS maps by performing a likelihood ratio test over the grid of possible coordinates, assuming a point source with a simple photon index $\Gamma = -2$ power law spectral fit. To find the best fit, we allowed the isotropic and Galactic diffuse background components as well as the sources with $TS \geq 10$ within 3° from the RoI center to vary in normalization. In order to find the most significant features, we used the iterative source-finding algorithm `gta.find_sources` in `fermipy` to locate emission peaks on the TS map. The most significant features ($TS \geq 9$) are labeled J1911.8+2044 and J1913.2+1901 (see Figure 2). As a final step, we used the `gta.localize_fermipy` subroutine to refine the position of each residual (see Table 1). The uncertainty listed corresponds to a radius of error ellipse at 68% confidence. Figure 2 shows $3^\circ \times 3^\circ$ pre-burst and post-burst TS maps centered on the GRB 221009A location after excluding J1911.8+2044 and J1913.2+1901 from the model. One can see that in both cases, the field is textured with several structures in the TS map.

The most significant feature in the TS map J1911.8+2044 is offset by 0.983° from the GRB 221009A position. γ -ray emission in this region appears to peak after the GRB trigger. However, as can be seen in the pre-burst TS map (Left Panel in Figure 2), there appears to be γ -ray emission in the proximity of J1911.8+2044 at $RA = 287^\circ.764 \pm 0.053$, $Dec = 20.652 \pm 0.054$. Since we cannot unequivocally rule out γ rays potentially produced prior to the GRB onset at this location, we discard the possibility that J1911.8+2044 was induced by GRB 221009A.

The other residual of interest is J1913.2+1901, which is located 0.75° from GRB 221009A. It also coincides with a 664.6 GeV event that arrived approximately 191.9 days after the GBM trigger. No other event above 100 GeV has been observed within 0.5° of the J1913.2+1901 position during the *Fermi* mission prior to GRB 221009A (approximately 14.2 years). The total 95% PSF containment radius for a 664.6 GeV event is about 0.3° . Thus, the residual appears disjointed from GRB 221009A and most likely outside the host galaxy. Assuming a power law with photon index $\Gamma = -2$, the LAT upper limits (95% confidence level, 100 GeV – 1 TeV) is $\leq 2.3 \times 10^{-11} \text{ erg cm}^{-2} \text{ s}^{-1}$ over 5.73–456.69 days after the GBM trigger. We choose to provide 95% confidence level upper limits throughout the paper since the $TS \leq 25$. Analysis of the same region 14.2 years prior to GRB 221009A indicates a pre-burst flux upper limit $\leq 1.5 \times 10^{-12} \text{ erg cm}^{-2} \text{ s}^{-1}$ at the same location.

To find a potential bright counterpart near this region, we searched the High Energy Astrophysics Science Archive Research Center (HEASARC) archives for possible known blazars. Unfortunately, no remarkable candidate sources within 0.15° of J1913.2+1901 exist. Generally, a GeV-producing blazar tends to be quite prominent in other wavelengths. The only cataloged X-ray source nearby is 2RXS J191301.9+190807, which appears to be an unrelated coronal emitting star based on its optical counterpart. Unfortunately, this region of the sky is not included in the eROSITA Early Data Release¹. In light of its uncertain origin, we consider a scenario whereby GRB 221009A induced the late γ -ray emission from J1913.2+1901.

¹<https://erosita.mpe.mpg.de/edr/eROSITAObservations/ConeSearch/>

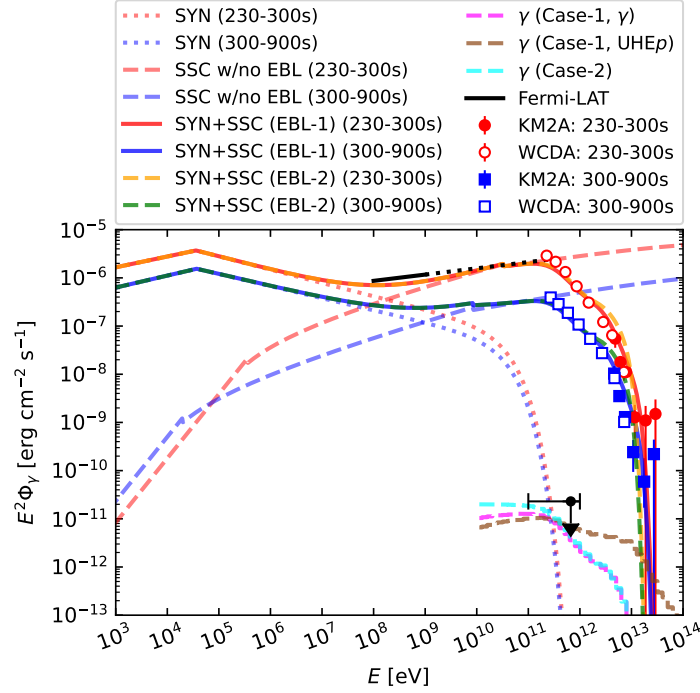


Figure 3. UHE proton-induced and UHE/VHE γ -ray induced cascade γ -ray flux shown together with LHAASO detection [2], *Fermi*-LAT detection in the 0.1-1 GeV range, and *Fermi*-LAT flux upper limit in the 100 GeV - 1 TeV range calculated for a period of 5.73-456.69 days after the GRB 221009A trigger. The synchrotron and SSC models were calculated following Refs. [11, 15, 16] with parameters: $E_k = 10^{55}$ erg, $\Gamma_0 = 500$, $n_0 = 10^{-2}$ cm $^{-3}$, $p = 2.5$, $\epsilon_e = 4 \times 10^{-3}$ and $\epsilon_B = 10^{-3}$. The EBL-1 and EBL-2 models are by Finke et al. [17] and Dominguez et al. [18], respectively. The filled black circle with downward arrow represents the 664.6 GeV photon detected by *Fermi*-LAT 191.9 days post-burst. The dashed magenta and brown curves correspond to UHE proton-induced cascade emission components from the structured region and intergalactic regions, respectively. The cyan dashed curve, on the other hand, corresponds to cascade emission from the VHE γ -rays injected from the GRB.

3 Potential Explanations

VHE emission detected from a handful of GRBs [19–21] are typically modeled using SSC emission by relativistic electrons in an external forward shock, see e.g., [15, 16, 22–28]. TeV emission detected by LHAASO from GRB 221009A can also be modeled as SSC emission [2, 11, 29–34]. In Figure 3, we show such a fit with GRB afterglow model parameters, e.g., the isotropic-equivalent kinetic energy of the blast wave, $E_k = 10^{55}$ erg [2], the initial bulk Lorentz factor of the GRB fireball, $\Gamma_0 = 500$, the density of the interstellar medium, $n_0 = 10^{-2}$ cm $^{-3}$, the power-law index of shock-accelerated electrons' energy distribution, $p = 2.5$, the fraction of shock energy going into the electrons, $\epsilon_e = 4 \times 10^{-3}$, and the fraction of shock energy going into the magnetic field, $\epsilon_B = 10^{-3}$ [11, 15]. Note that a different set of parameter values can also give a satisfactory fit to data due to the degeneracy among model parameters. Furthermore, the SSC spectrum shown (dashed lines) is in the Thomson regime, and it will undergo a break at ≈ 0.5 TeV due to the Klein-Nishina effect [15, 35]. The spectrum is therefore, $dn/d\epsilon_\gamma \propto \epsilon_\gamma^{-1.5}$ for $\epsilon_\gamma \lesssim 0.5$ TeV and $\propto \epsilon_\gamma^{-p} \propto \epsilon_\gamma^{-2.5}$ for $\epsilon_\gamma \gtrsim 0.5$ TeV. The SSC fluxes fitting LHAASO data [2] during the time intervals $T_0 + (230 - 300)$ s and $T_0 + (300 - 900)$ s are shown in Figure 3 by orange-dashed and blue-dashed curves,

respectively. The orange-dotted and blue-dotted curves indicate the synchrotron spectrum for the two intervals. The orange solid and blue solid curves represent the total leptonic emission spectrum with EBL attenuation due to the Finke et al. [17] model (EBL-1). We also show the total spectrum for Dominguez et al. [18] EBL model (EBL-2) by yellow dashed and green dashed lines for the two distinct time intervals.

While VHE emission detected from GRBs is dominated by SSC in the forward shock of a GRB blast wave, the SSC flux typically declines as $F_\nu \propto t^\alpha$. In the case of a constant density interstellar medium (ISM), we have $\alpha = -(9p - 10)/8$, and in the case of a wind-type medium $\alpha = -p + 1$, both for the observed emission above the peak of the SSC spectrum in the Thomson regime, see, e.g., [15]. For $p \approx 2$, the index for the electron energy distribution, $\alpha \approx -1$. The flux decay observed by LHAASO in the 0.2–5 TeV range is $\alpha_{2,\text{TeV}} = -1.115 \pm 0.012$ in their second time interval of $\approx T_0 + 230$ s to $\approx T_0 + 670$ s [2]. However, LHAASO also observed a further steepening of the flux at $\gtrsim T_0 + 670$ s with a flux-decay index $\alpha_{3,\text{TeV}} = -2.21^{+0.30}_{-0.83}$. If interpreted as the post-jet-break decay [36], for which $F_\nu \propto t^{-p}$ and for $p \approx \alpha_{3,\text{TeV}}$, the 0.2–5 TeV flux at $T_0 + 191.9$ day would be $\approx 3 \times 10^{-7} (191.9 \text{ day}/670 \text{ sec})^{\alpha_{3,\text{TeV}}} \sim (3 \times 10^{-13} - 3 \times 10^{-18}) \text{ erg cm}^{-2} \text{ s}^{-1}$, which is well below the *Fermi*-LAT flux upper limit shown in Figure 3 and cannot explain the detection of the 664.6 GeV photon. Therefore, this paper explores possible scenarios to account for such an energetic photon, considering its long delay and offset from the GRB position.

3.1 UHE proton-induced cascade emission

The comoving distance to GRB 221009A is ≈ 648 Mpc ($z = 0.151$), and an angular offset of 0.75° corresponds to a transverse distance of 8.5 Mpc. Such a separation corresponds to filament, galaxy-cluster, or magnetic void scales. A potential model is similar to the one proposed in Ref. [13] where the GRB is embedded in the large-scale structure. However, here, we model γ -ray emission from cascades. We consider that the host galaxy of GRB 221009A is embedded in a magnetized cosmological volume with a length scale of $d_c \approx 5$ Mpc and magnetic field strength of $\sim 0.01 - 1 \mu\text{G}$ [37] with a coherence length of $\lambda_c \approx 10 - 100$ kpc. In this work, we take a conservative value of $B_{\text{SR}} = 10$ nG. For Larmor radius r_L in the magnetic field, the expected deflection angle, $\theta_{\text{df}} = \sqrt{2d_c\lambda_c}/3r_L$ for UHECR with charge Z from the GRB direction can be written as [38, 39]

$$\theta_{\text{df}} \simeq 0.53^\circ Z \left(\frac{d_c}{5 \text{ Mpc}} \right)^{1/2} \left(\frac{\lambda_c}{10 \text{ kpc}} \right)^{1/2} \left(\frac{B_{\text{SR}}}{10 \text{ nG}} \right) \left(\frac{\varepsilon_{\text{UHE}p}}{100 \text{ EeV}} \right)^{-1} \quad (3.1)$$

The observed 0.75° offset of the 664.6 GeV from the position of the GRB 221009A could originate from the accelerated UHECR protons that escape from the GRB and interact in the structured region if $B_{\text{SR}} \approx 10$ nG. The time delay induced by the deflection in the magnetized structure can be expressed as [40, 41]

$$\Delta t_{\text{SR}} \simeq \frac{d_c \theta_{\text{df}}^2}{2c} \simeq 0.7 \times 10^3 \text{ yrs} \left(\frac{d_c}{5 \text{ Mpc}} \right)^2 \left(\frac{\lambda_c}{10 \text{ kpc}} \right) \left(\frac{B_{\text{SR}}}{10 \text{ nG}} \right)^2 \left(\frac{\varepsilon_{\text{UHE}p}}{100 \text{ EeV}} \right)^{-2}. \quad (3.2)$$

Any deflection in the intergalactic medium (IGM) in the void region is very small for the current constraints on the extragalactic magnetic field of $\lesssim 10^{-14}$ G [42, 43].

However, there is an additional time delay due to the formation and emission of the leptonic cascade particles. An analytic expression for the time delay in cascade emission

in the void IGM may depend on the inverse Compton (IC) cooling time scale of electron-positron pairs on the CMB photons, $t_{\text{IC}} = 3m_e c / (4\gamma_e \sigma_{\text{T}} u_{\text{CMB}}) \simeq 4.2 \times 10^{12} (\gamma_e/10^7)^{-1}$ s at $z = 0.151$, where γ_e is the electron Lorentz factor and u_{CMB} is the blackbody CMB photon energy density at $z = 0.151$, see, e.g., [44–46]. The deflection angle of the pairs in the IGM can be calculated from a ratio between the IC path and the Larmor radius $R_{\text{L}} = \gamma_e m_e c^2 / e B_{\text{IGM}}$, which is given by $\theta_B \approx ct_{\text{IC}} / R_{\text{L}} \simeq 7.4 \times 10^{-2} (\gamma_e/10^7)^{-2} (B_{\text{IGM}}/10^{-14} \text{ G})$. For a pencil beam, the corresponding time delay due to the bending of the electron trajectory in the magnetic field is $\Delta t_B \approx t_{\text{IC}} \theta_B^2 / 2 \simeq 360 (\gamma_e/10^7)^{-5} (B_{\text{IGM}}/10^{-14} \text{ G})^2$ yrs. However, the beam has a finite angular spreading in reality, leading to $\Delta t_B \approx \lambda_{\gamma\gamma} \theta_B^2 / (2c) \simeq 3.5 \times 10^5 (\gamma_e/10^7)^{-4} (B_{\text{IGM}}/10^{-14} \text{ G})^2$ yrs [47–49], where $\lambda_{\gamma\gamma} \sim 200 (n_{\text{CIB}}/0.01 \text{ cm}^{-3})$ Mpc and n_{CIB} is the local number density of cosmic infrared photons. One requires $\gamma_e \sim 3 \times 10^7$ to upscatter a CMB photon to 665 GeV. This corresponds to a time delay of ~ 1.5 yrs, with other parameters unchanged. A similar calculation can be performed for the time delay in the structured region with $B_{\text{SR}} = 10$ nG, and $\gamma_e = 10^9$ (for e^\pm produced by 1 EeV UHECRs, the lowest energy in our simulations, due to the BH process). The time delay would be $\sim 3.5 \times 10^5$ yrs in that case.

3.1.1 Simulation setup

We use the CRPROPA 3.2 code [50, 51] for the propagation of UHECRs and for calculating γ rays from their interactions. There are two zones in our setup, viz., (i) the structured region with a strong magnetic field extending up to a radius of 5 Mpc where the GRB is embedded and (ii) the intergalactic medium that extends from the edge of the structured volume to Earth and is mostly dominated by voids with a weak magnetic field.

A root mean square (RMS) magnetic field $B_{\text{SR}} = 10$ nG with 10 kpc coherence length is considered for the structured region [38, 52, 53]. To propagate the UHECRs through the magnetized cosmological structure, we create a random realization of a turbulent magnetic field given by a Kolmogorov power spectrum on 20–25 kpc length scales. The field is stored on a 512^3 grid with 10 kpc grid spacing and thus has an extent of $(512 \times 10 \text{ kpc})^3$. The secondary cosmic rays and γ rays produced in the structured region are further propagated through the intergalactic medium and collected at Earth. The intergalactic medium is parametrized with an RMS field strength $B_{\text{IGM}} = 1.82 \times 10^{-5}$ nG and 1 Mpc coherence length [11]. The magnetization for this region is also given by a turbulent field with Kolmogorov power spectrum defined over 0.1–5 Mpc length scales and is stored on a 256^3 grid with 30 kpc grid spacing. The field is periodically repeated in space to cover an arbitrary volume.

Tracing the direction of γ rays produced in electromagnetic cascades induced by UHECRs is computationally expensive in Monte Carlo simulations. We have propagated secondary electrons and γ rays separately and assumed that the UHECRs deflected away from the angular region of interest do not contribute to the signal. The secondary electrons lose energy fast enough to undergo significant deflection. Using a 1-D simulation, we calculate the secondary cascade flux and study their deflections using a 3-D simulation. We inject UHECR protons from the GRB jet with $dN/dE \propto E^{-2}$ spectrum in the 1-100 EeV energy range, directed towards our line of sight. 1-D simulations provide the isotropic fluxes of cosmic rays and γ rays produced via photohadronic interactions and electromagnetic cascades during propagation. We include all energy loss processes, viz., photopion production, Bethe-Heitler pair production, and adiabatic energy loss due to expansion of the Universe, for UHE protons interacting with the CMB and EBL photons, as well as nuclear β -decay for neutrons. The electromagnetic cascade considers Breit-Wheeler pair production, double and triplet pair production,

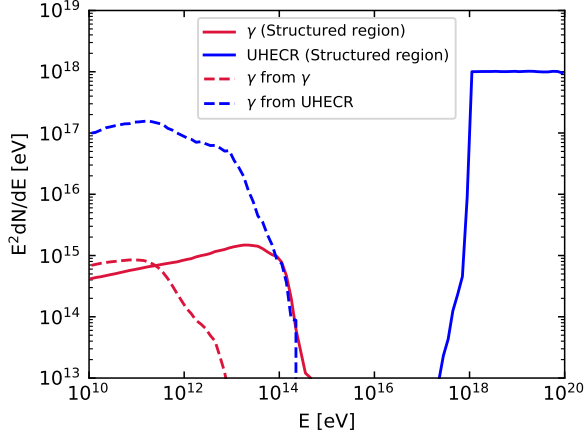


Figure 4. Protons with a spectrum $dN/dE \propto E^{-2}$ and energy between 1–100 EeV are injected from the GRB jet. γ rays (red solid line) and secondary UHECR flux (blue solid line) are produced via UHECR interactions, followed by electromagnetic cascades over a 5 Mpc length scale in the structured region with RMS magnetic field strength of 10 nG. Cosmogenic γ -ray flux arriving at Earth from the cascade of these secondary γ rays and secondary UHECR spectrum is shown by a red dashed line and blue dashed line, respectively. An arbitrary normalization factor is applied such that all spectra represent a single UHE proton injection at the source.

inverse-Compton scattering of background photons, and synchrotron radiation in the cosmic magnetic fields.

3-D simulations, including deflection in cosmic magnetic fields, are utilized to estimate the angular distribution of UHECRs at various points of observation, viz., the edge of the magnetized cosmological structure and Earth. We make the approximation that the angular deflection distribution of secondary γ -rays mimics the distribution of UHECR arrival directions. We use the survival fractions of UHE protons in the two zones to obtain the UHE proton energy in the source from the γ -ray flux normalization, see e.g., Ref. [54]. We discuss this in Subsec. 3.1.2. Due to computational constraints, we calculate the cascade photon flux down to 10 GeV energies. At lower energies, uncertainties in the flux arise due to discrepancies in energy conservation and the numerical methods employed in the literature, see e.g., Refs. [55, 56]

3.1.2 Propagation in structured regions

We perform a 1-D simulation to collect secondary γ rays at the edge of the structured region and calculate the resulting cosmogenic γ -ray spectrum from the electromagnetic cascade initiated by secondary e^\pm and γ rays. This is done using the Monte Carlo approach in CR-PROPA 3.2 [50, 51]. Figure 4 shows the isotropic γ -ray spectrum (red solid curve) and the UHECR spectrum (blue solid curve) emerging from the structured region after propagation. Since 4-D simulations of the electromagnetic cascade are computationally expensive to perform using CRPropa, we assume the secondary particles propagate long enough to traverse the 5 Mpc distance at the edge of the structured region. The spectra we show in Figure 4 are integrated over propagation time corresponding to this distance, and the injection time period does not affect these energy fractions. The fluxes are presented in arbitrary units normalized for a single UHE proton injection from the GRB jet. The γ -ray flux falls off sharply beyond 10^{14} eV. A small fraction of the UHE proton energy goes into the production of these

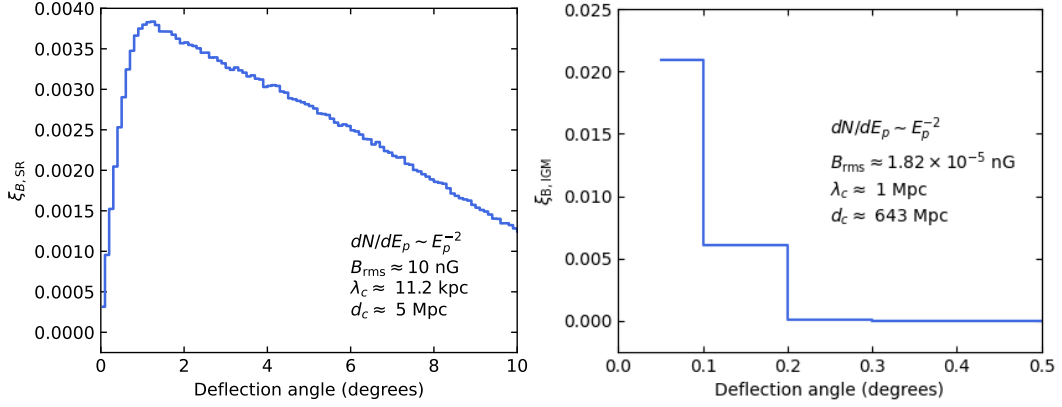


Figure 5. *Left:* Distribution of the UHECR fraction as a function of the deflection angle after propagating through the structured region, mapped on the surface of a sphere centered 5 Mpc from the GRB with a radius of 0.5 Mpc. *Right:* Survival fraction of UHECRs injected from a magnetized cosmological volume after propagating through the intergalactic medium (IGM), measured on the surface of an observer sphere centered on Earth with a radius of 1 Mpc.

secondary γ rays.

The strong magnetic field in the structured region deflects the UHECRs from their initial direction along our line of sight. The deflection of UHECRs is studied using a separate 3-D simulation of UHECR propagation in the same magnetic field as described earlier but with a conical emission directed towards Earth with a half opening angle of 0.8° . The latter corresponds to the GRB jet opening angle as predicted by the LHAASO collaboration [2]. The propagated UHECR events are collected using an observer sphere with a radius of 0.5 Mpc located at a distance of 5 Mpc from the location of GRB 221009A, assumed to be a point source. The fraction of UHECRs arriving on the surface of this sphere for angular deflection bins of 0.1° is shown in the left panel of Figure 5, and is denoted by $\xi_{B,SR}$. The deflection peaks at around 1° for the chosen magnetic field configuration of the cosmological structured region. It should be noted that the deflection on short angular scales varies depending on the length scales and grid size used in the simulations to define the turbulent magnetic field.

3.1.3 Propagation in void regions

The secondary γ ray and UHECR spectra emerging from the structured region are further propagated through the intergalactic medium. Again, a 1-D simulation is performed to collect the cosmogenic γ rays at Earth. The resultant γ -ray flux is the sum of events produced from the propagation of γ rays produced in the structured volume and that from the propagation of secondary UHECRs. The isotropic fluxes of the individual components arriving at Earth are shown in Figure 4. We find that the contribution of the γ -ray flux emerging from the structured region to the final cosmogenic γ -ray flux at Earth (red dashed curve) is subdominant compared to that from UHECRs (blue dashed curve) by almost two orders of magnitude. To increase the simulation efficiency in calculating electromagnetic cascades, a threshold energy of 10 GeV is used, as before, for the break condition in the simulations.

To calculate the survival fraction of UHECRs on Earth after propagation through the IGM, we use a conical injection at the edge of the structured region, which is the initial point of our second zone. The choice of our angular width of the injection is inspired by trial simulations, which show that no particles are observed at Earth for initial emission direction

at an angle $\gtrsim 0.55^\circ$ away from our Galaxy. UHECR events arriving at Earth on the surface of an observer sphere of radius 1 Mpc, centered at Earth, are binned in 0.1° intervals and denoted by $\xi_{B,\text{IGM}}$. This is shown in the right panel of Figure 5. The flux of secondary γ rays at Earth from UHECRs injected from the structured region into the IGM is then obtained by multiplying the flux with $\xi_{B,\text{IGM}}(\theta < 0.75^\circ) \times \xi_{B,\text{SR}}(\theta < 0.55^\circ)$.

However, for the γ -ray flux arising from secondary γ rays injected into the intergalactic medium at the edge of the structured region, no further deflection is assumed, and the angular distribution at Earth can be approximated as that given in the left panel of Figure 5. We find that although the observed flux contained within 0.75° of the initial emission direction is assumed to account for the late photon observation, the right panel of Figure 5 shows that the flux of γ rays produced from UHECR propagation in the IGM is negligible within this angular deflection bin. Hence, the late photon observation by *Fermi*-LAT is assumed to originate from secondary γ -rays injected from the structured region, and these photons do not undergo any further deflection during their propagation through the IGM.

3.1.4 Broadband spectrum and energy requirement

In Figure 3, we show the multi-wavelength spectrum of GRB 221009A for our synchrotron and SSC emission model during 230-300 s after the *Fermi*-GBM trigger, assuming that the blastwave is already in decelerating phase during this time interval. We highlight the intrinsic and EBL-absorbed spectra for the EBL models by Finke et al. [17] (EBL-1) and Dominguez et al. [18] (EBL-2). The γ -ray flux coming from secondary γ rays (dashed magenta line) and secondary UHECRs (dashed brown line) injected by the structured region into the IGM are also shown in Figure 3. In our model, the photon flux at Earth coming from the secondary photons produced in the structured region gives rise to the late photon observed by *Fermi*-LAT. The electromagnetic cascade of these photons coming from an annular region at 0.75° and of angular width, 0.3° (including the two bins of width 0.15° on either side of the bin corresponding to the deflection) gives the predicted γ -ray spectrum. However, for the calculation of required energy in UHE protons in this model, we consider the entire flux contained within $0^\circ - 0.75^\circ$ angular region.

The fraction of cosmic-ray energy injected by the GRB that goes into the γ -ray flux indicated by the magenta dashed curve in Figure 3 is $f_{\gamma,p}^{\text{SR}} = 6.75 \times 10^{-4}$, which is calculated from the γ -ray flux (red dashed curve) in Figure 4. The fraction of UHE protons within 0.9° of the initial emission direction at the edge of the structured region is $\xi_{B,\text{SR}}(\theta < 0.9^\circ) \approx 2.1 \times 10^{-2}$ (see Figure 5 left panel). The angular range corresponds to the observed offset, including the angular uncertainty of 0.15° in the observation of photons > 30 GeV by *Fermi*-LAT. Here, our choice of the deflection angle range is due to *Fermi*-LAT's resolution of 0.15° to photons of energy > 30 GeV. The following expression then finds the required total proton energy considering a steady γ -ray spectrum,

$$E_{\text{UHE}p} \gtrsim \frac{2\pi d_L^2 (1 - \cos \theta_j)}{\xi_{B,\text{SR}} f_{\gamma,p}^{\text{SR}}} \int_{10 \text{ GeV}}^{100 \text{ EeV}} \int_{T_0}^T \varepsilon_\gamma \frac{dn}{d\varepsilon_\gamma dA dt} d\varepsilon_\gamma dt. \quad (3.3)$$

where $T = 191.9$ days is the time corresponding to the detection of 664.6 GeV photon, and ε_γ is the photon energy of resultant γ -ray spectrum. The injection time of the protons can be much shorter than T . Here, the integration is over the flux of cosmogenic γ -ray flux originating from secondary photons injected by the galaxy cluster region into IGM. This flux is required to explain the *Fermi*-LAT observation (shown by black data point), as the cosmogenic γ -ray flux from secondary UHECRs is negligible at an angular offset of 0.75° . The factor in the

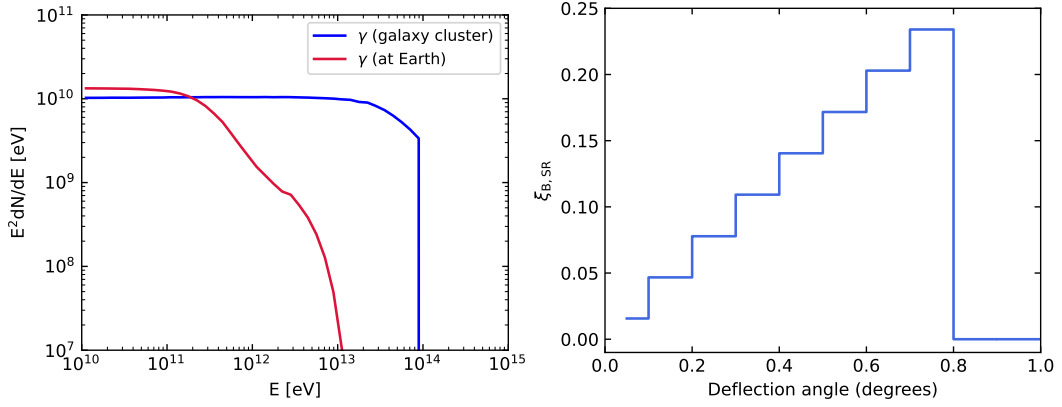


Figure 6. *Left:* The unattenuated SSC flux is approximately given by a γ -ray spectrum $dn/d\varepsilon_\gamma \propto \varepsilon_\gamma^{-2}$ in the 0.1 – 100 TeV range, is injected from the GRB into the structured region. The blue solid line indicates the secondary γ -ray spectrum after propagation in the medium of the cosmological structure, and the red solid line indicates the isotropic γ -ray spectrum at Earth. The flux is normalized to a single γ photon injection at the source. *Right:* Distribution of observed cascade photons in various angular deflection bins. A sharp cutoff at 0.8° is due to the GRB jet opening angle considered in the simulations.

numerator $2\pi d_L^2(1 - \cos\theta_j)$ is the area subtended by the GRB jet at the distance of the observer. For a jet-opening angle of $\theta_j \sim 0.8^\circ$, inferred from the jet-break at TeV energies by LHAASO [2], we find the total energy in protons in the GRB jet to be $E_{\text{UHE}p} \sim 6 \times 10^{52}$ erg, which corresponds to an isotropic equivalent energy release of $E_{\text{UHE}p}^{\text{iso}} \sim 10^{57}$ erg. The energy requirement for protons sets the normalization for the cosmogenic γ -ray flux from secondary UHECRs (brown dashed line in Figure 3). This flux is calculated using an expression similar to Eq. (3.3), but using an angular deflection factor $\xi_{B,\text{IGM}}(\theta < 0.75^\circ) \times \xi_{B,\text{SR}}(\theta < 0.55^\circ)$, as described in Sec. 3.1.3. Additionally, the factor $f_{\gamma,p}^{\text{SR}}$ is replaced by $f_{\gamma,p}^{\text{SR+IGM}}$ that corresponds to the fraction of injected UHECR energy from the GRB that goes into this component of γ -ray flux.

3.2 UHE/VHE γ -ray-induced cascade emission

As described in the Introduction, VHE γ rays emitted directly from the GRB jet should have declined at the time of a 664.6 GeV photon detection. In addition, as shown in the previous section, the required energetics in the UHE proton-induced γ -ray scenario is too demanding. Therefore, as an alternative scenario that is energetically acceptable, we suggest the scenario in which the observed high-energy photon originates from VHE γ rays. Such VHE γ -ray emission can be realized in two ways. First, UHE γ rays produced during the prompt emission [45, 57] or the early afterglow phase [58–60] can escape from the strongly-magnetized GRB jet and are cascaded inside the structured region. The pairs produced quickly lose their energies via synchrotron emission “while they are strongly beamed”. The resulting “synchrotron pair echo” [13], which is synchrotron emission induced by UHE pairs, uniquely predicted a time delay of ~ 100 days at $\varepsilon_\gamma \sim 0.3 - 1$ TeV. Indeed, from Eq. 4 of Ref. [13], we have

$$\Delta t_{\text{syn}} \approx \frac{\min[\lambda_{\gamma\gamma}, d_c] \theta_{\text{syn}}^2}{2c} \simeq 140 \text{ days} \left(\frac{\min[\lambda_{\gamma\gamma}, d_c]}{5 \text{ Mpc}} \right) \left(\frac{\varepsilon_\gamma}{600 \text{ GeV}} \right)^{-2}. \quad (3.4)$$

Thus, if the injected isotropic-equivalent UHE γ -ray energy is $E_{\text{UHE}\gamma}^{\text{iso}} \sim 10^{53}$ erg, which is only $\sim 1\%$ of the observed isotropic-equivalent γ -ray energy, the synchrotron luminosity at $\sim 0.3 - 1$ TeV is $\sim 10^{46}$ erg s $^{-1}$, being consistent with the observation of a 664.6 GeV photon. In this case, for our purpose, it is sufficient to consider GeV-TeV γ rays as the injected primaries, following a similar approach to the analysis in Sec. 3.1. For simplicity, we inject a $dn/d\varepsilon_\gamma \propto \varepsilon_\gamma^\Gamma$ spectrum in the 0.1–100 TeV range in CRPropa. In this work we use $\Gamma = -2$, which may mimic the spectrum of synchrotron pair echo emission that is formed while UHE γ -rays propagate through the intergalactic medium (IGM) in structured magnetized regions such as galaxy clusters and filaments. The spectrum of EBL-unattenuated γ -ray flux is similar to the blue-dashed line plotted in Figure 3.

The second case is VHE emission produced by the GRB jet powered by a long-lasting central engine. As a reference spectrum used in our CRPropa simulation, we use the spectrum based on the SSC modeling of the LHAASO data, which is indicated by the blue dashed line in Figure 3). In this case, the corresponding isotropic-equivalent VHE γ -ray luminosity can be calculated as $L_{\text{VHE}\gamma}^{\text{iso}} = 4\pi d_L^2 \int d\varepsilon_\gamma \varepsilon_\gamma dn/d\varepsilon_\gamma \sim 2 \times 10^{50}$ erg s $^{-1}$. Now assuming a duration of ~ 1000 s, the isotropic-equivalent injected energy is $E_{\text{VHE}\gamma}^{\text{iso}} \sim 2 \times 10^{53}$ erg. Assuming a constant t^{-1} decay as expected in the SSC model, the VHE γ -ray luminosity at the time of the late photon observation is estimated to be $\sim 10^{46}$ erg s $^{-1}$. A fraction of the injected energy goes into the cascade photons. Note that in the case of a t^{-2} decay as expected if the jet-break detected by LHAASO is correct, the expected flux ~ 100 days after the burst detection would be too low to explain the observation, as mentioned earlier in Sec. 3. Thus, the GRB afterglow scenario would not be viable and late-time injection is necessary if VHE emission is attributed to the GRB jet.

In the VHE γ -ray scenario, VHE γ -rays, which can be produced as secondary synchrotron emission produced inside the magnetized structures [13], must eventually escape into the void region and should further be cascaded through $\gamma\gamma$ pair production with cosmic background photons, including CMB and EBL photons, as well as IC scattering of background photons by high-energy electrons and positrons. This is generally known as “inverse-Compton pair echo” emission [48] as this cascade emission sustains for a longer duration than injection at source due to deflection of the electron-positron pairs in the intergalactic magnetic field (IGMF) in the void region, even after the original emission from the GRB ceases [45–47, 49, 61, 62]. Detection of such delayed emission can probe the void IGMF strength, and non-detection of such a component from GRB 221009A resulted in a void IGMF lower bound of 10^{-19} G [63]. However, we consider the same parameters for the magnetic field in the structured region and the void region as were considered in the previous scenario.

The left panel of Figure 6 shows the isotropic γ -ray spectrum in $\varepsilon_\gamma^2 dn/d\varepsilon_\gamma$ units at the edge of the structured region (blue solid line) and that on Earth (red solid line) due to the propagation and electromagnetic cascade of injected photons. The spectra are normalized to represent a single photon injection at the source. Due to computational limitations, we simulate the cascade spectrum down to 10 GeV only. Again, we perform a 3-D simulation with a conical injection, having an opening angle 0.8° , corresponding to the jet opening angle. We calculate the fraction of secondary photons in angular bins of 0.1° from the initial emission direction. An observer sphere of radius 0.5 Mpc is used to collect the secondaries at the edge of the structured region. The normalization of the survival fraction is fixed on energy conservation requirements.

The right panel in Figure 6 shows the angular distribution of secondary photons at the edge of the structured region. About 99% of photons from the cascade in the output energy

range is within this angular range. However, since the electromagnetic cascade can increase the number of observed photons than injected, and also since we do not consider photons produced below 10 GeV, we use the factor $\xi_{B,\text{SR}}$ to be the fraction of energy within this angular range with respect to the injected energy. We find that this fraction is 0.89. Since the magnetic field of the void region is much lower, and photons are not significantly deflected, we consider deflections only due to the structured region. But these photons undergo further cascades in the void region. The fraction of γ -ray energy injected from the structured region into the IGM that goes into the electromagnetic cascade flux at Earth within 0.01 – 100 TeV is $f_{\gamma,\text{IGM}} \approx 0.56$. In this case, we also assume that the secondary γ -rays are produced in the structured region (shown by the blue line in the left panel of Figure 6) in the annular region at an angle 0.8° and a width of $\pm 0.15^\circ$. Using these values and a similar expression, as in Equation (3.3), we find the required isotropic-equivalent luminosity in primary γ rays to be $\sim 10^{46} \text{ erg s}^{-1}$.

4 Calculation of the expected number of events

To ensure that our theoretical models do not over-predict the observed data, we performed a cross-check by assuming a simple power-law model $dn/d\varepsilon_\gamma \propto \varepsilon_\gamma^\Gamma$ and calculating the exposure in four energy bands (from 1–, 10–, 100–, and 600 GeV– to 1 TeV) during the time period $T_0 + 5.73$ days to $T_0 + 457.0$ days, for spectral indices $\Gamma = -2.5$ (Model a) and $\Gamma = -2.0$ (Model b). For each case, we determined the flux required to produce exactly one expected event between 100 GeV and 1 TeV, and then we computed the expected number of events (N_{exp}) in all four energy bands. These results were compared with the observed number of events (N_{obs}). The table below summarizes N_{obs} , N_{exp} , and the probability of observing N_{obs} given N_{exp} .

We also tested a broken power-law model ($\Gamma_1 = -1.8$ for $E < 140$ GeV, $\Gamma_2 = -2.3$ for $E \geq 140$ GeV; Model c), representative of the cascade model in Figure 3, and the same model, but calculating the exposure between $T_0 + 100$ days to $T_0 + 457.0$ days (Model d). A single power law with $\Gamma = -2.0$ was consistent with the observations, while softer indices ($\Gamma > -2.0$) overpredicted the counts below 100 GeV. The broken power-law model also agreed well with the data, predicting fewer events below 100 GeV while maintaining a reasonable probability of observing events above 600 GeV. Very similar results are obtained when computing the exposure starting from 100 days after the trigger, which is a proxy for cascade flux increasing sharply with time.

5 Summary and Conclusions

In this paper, we have studied the γ -ray emission J1913.2+1901 (TS ~ 10.6) detected by *Fermi*-LAT approximately 191.9 days after the trigger of GRB 221009A. The γ -ray emission, however, has a 0.75° offset from the location of the GRB. Such a large-angle deflection is intriguing given the angular resolution of *Fermi*-LAT is $\approx 0.1^\circ$ at $E > 10$ GeV, and begs an explanation.

While the γ -ray source could be unrelated to GRB 221009A, we discussed that the GRB exploded in a cosmological structured region with ≈ 5 Mpc radius and ≈ 10 nG magnetic field. UHECRs accelerated in the GRB jet propagate in structured regions of the IGM to produce secondary cascade emission by interacting with the EBL and CMB photons. Deflection of the UHECRs and hence of the cascade γ rays in the structured region could explain an

Energy Band	N_{obs}	N_{exp}	$P(N_{\text{obs}} N_{\text{exp}})$
Model a: Interval from $T_0+5.73$ d to $T_0+457.0$ d, $\Gamma=-2.5$			
1 GeV – 1 TeV	716	865.02	$< 10^{-5}$
10 GeV – 1 TeV	24	32.6	2.8×10^{-4}
100 GeV – 1 TeV	1	1	3.7×10^{-1}
600 GeV – 1 TeV	1	0.035	3.4×10^{-2}
Model b: Interval from $T_0+5.73$ d to $T_0+457.0$ d, $\Gamma=-2$			
1 GeV – 1 TeV	716	86.5	$< 10^{-5}$
10 GeV – 1 TeV	24	11.1	2.8×10^{-4}
100 GeV – 1 TeV	1	1	3.7×10^{-1}
600 GeV – 1 TeV	1	0.069	6.6×10^{-2}
Model c: Interval from $T_0+5.73$ d to $T_0+457.0$ d, $\Gamma_1=-1.8$, $\Gamma_2=-2.3$			
1 GeV – 1 TeV	716	56.1	$< 10^{-5}$
10 GeV – 1 TeV	24	10.5	7.7×10^{-5}
100 GeV – 1 TeV	1	1	3.7×10^{-1}
600 GeV – 1 TeV	1	0.047	4.5×10^{-2}
Model d: Interval from T_0+100 d to $T_0+457.0$ d, $\Gamma_1=-1.8$, $\Gamma_2=-2.3$			
1 GeV – 1 TeV	576	57.1	$< 10^{-5}$
10 GeV – 1 TeV	22	10.1	4.4×10^{-4}
100 GeV – 1 TeV	1	1	3.7×10^{-1}
600 GeV – 1 TeV	1	0.047	4.5×10^{-2}

Table 2. Poisson probability of observing N_{obs} events given N_{exp} expected events in four different energy bands and for four different models.

angular offset and corresponding extended VHE emission from GRB 221009A. Note that for our assumed value of 1.82×10^{-5} nG for the magnetic field in the void region, the deflection angle is only $\lesssim 0.2^\circ$. Such a deflection in the void region cannot explain the 0.75° offset of the 665.6 GeV photon. We have also explored the delay timescale for the cascade emission using analytic estimates, resulting in $\gtrsim 10^3$ yrs. The isotropic-equivalent energy required for cosmic-ray protons to power the cascade emission is $\sim 10^{57}$ erg. This corresponds to a factor $\gtrsim 50$ times more energy released in UHE protons over the time scale of the late photon detection compared to the isotropic-equivalent energy released in γ -rays [7].

The second scenario that we have considered is VHE γ -ray emission, which may be produced in structured regions through synchrotron emission. It was shown that the contribution of synchrotron pair echo is typically dominant over the contribution of UHE proton-induced cascade emission due to long time delays in the latter case [13]. While this scenario has difficulty in explaining the large offset, the required power for explaining the cascade emission is less demanding, which corresponds to only $\sim 1\%$ of the isotropic-equivalent γ -ray energy. It has been shown that the SSC emission can largely explain the observed LHAASO data, although other emission mechanisms such as proton synchrotron emission and $p\gamma$ interactions may contribute to the 10 TeV flux. Such afterglow emission decays as t^{-1} or even more rapidly in the presence of the jet break. Therefore, the afterglow emission itself would not provide enough power to produce the required flux to explain the late photon, and additional energy injection might be necessary.

We have also performed an independent check on the expected number of events between 0.1 – 1 TeV 5.73 days after the burst using various flux shapes (power-law and broken power-

law) and time intervals (5.73 days and 100 days after the burst). We found that the UHE proton-induced or UHE/VHE γ -ray-induced cascade flux, approximated by the broken power laws, does not over-produce VHE events in the LAT.

Extragalactic propagation of UHECRs injected by the GRB jet produces neutrinos peaking in the EeV range. No neutrino events were detected by either IceCube [64] or KM3NeT [65] coincident with this GRB. While internal shock acceleration is expected to yield PeV neutrinos via interactions with prompt γ -rays, their non-detection places a time-integrated upper limit mainly in the 0.8–1 PeV range. UHECRs may be accelerated in the external shock during the afterglow phase, where interactions with afterglow photons also produce neutrinos in the EeV range. The resulting flux remains well below the current IceCube sensitivity [66].

For a fixed magnetic field in the structured region, a larger jet opening angle of a few degrees, as inferred from radio and X-ray polarization [67–70], results in greater angular dispersion of UHECRs from the GRB. For our energy estimate, we compute the proton fraction within 0.9° of the initial emission direction, taking into account the Fermi-LAT angular resolution of 0.15° above 10 GeV. A larger θ_j reduces this fraction and thus increases the required proton energy.

Our results also have implications for the observation of VHE γ -rays from GRBs other than GRB 221009A. Future searches for delayed photons can be carried out after GRB triggers in *Fermi*-LAT data and ground-based γ -ray detectors. A stacking analysis can be performed from the directions of different GRBs to increase detection significance. Our modeling can be used to search for UHECR signatures through these delayed photons and to explore the environment of the GRB.

Acknowledgments

The *Fermi*-LAT Collaboration acknowledges generous ongoing support from a number of agencies and institutes that have supported both the development and the operation of the LAT as well as scientific data analysis. These include the National Aeronautics and Space Administration and the Department of Energy in the United States, the Commissariat à l’Energie Atomique and the Centre National de la Recherche Scientifique / Institut National de Physique Nucléaire et de Physique des Particules in France, the Agenzia Spaziale Italiana and the Istituto Nazionale di Fisica Nucleare in Italy, the Ministry of Education, Culture, Sports, Science and Technology (MEXT), High Energy Accelerator Research Organization (KEK) and Japan Aerospace Exploration Agency (JAXA) in Japan, and the K. A. Wallenberg Foundation, the Swedish Research Council and the Swedish National Space Board in Sweden.

We thank Guillem Martí-Devesa for carefully reading the manuscript and for providing helpful comments. This research by S.D. and K.M. is supported by KAKENHI No. 20H05852. The work of K.M. is supported by the NSF Grants No. AST-2108466, No. AST-2108467, and No. 2308021. The material is based upon work supported by NASA under award number 80GSFC24M0006. S.R. was partially supported by a BRICS STI grant and by a NITheCS grant from the National Research Foundation, South Africa. This research has made use of data obtained through the High Energy Astrophysics Science Archive Research Center Online Service, provided by the NASA/Goddard Space Flight Center. Numerical computation in this work was partly carried out at the Yukawa Institute Computer Facility, Kyoto University, Japan.

References

- [1] E. Burns, D. Svinkin, E. Fenimore, D.A. Kann, J.F. Agüí Fernández, D. Frederiks et al., *GRB 221009A: The Boat*, *Astrophys. J. Lett.* **946** (2023) L31 [2302.14037].
- [2] LHAASO collaboration, *A tera-electron volt afterglow from a narrow jet in an extremely bright gamma-ray burst*, *Science* **380** (2023) adg9328 [2306.06372].
- [3] LHAASO collaboration, *Very high energy gamma-ray emission beyond 10 TeV from GRB 221009A*, *Sci. Adv.* **9** (2023) adj2778 [2310.08845].
- [4] S. Lesage, P. Veres, M.S. Briggs, A. Goldstein, D. Kocevski, E. Burns et al., *Fermi-GBM Discovery of GRB 221009A: An Extraordinarily Bright GRB from Onset to Afterglow*, *Astrophys. J. Lett.* **952** (2023) L42 [2303.14172].
- [5] E. Bissaldi, N. Omodei and M. Kerr, *Grb 221009a or swift j1913.1+1946: Fermi-lat detection*, *GCN Circ.* **32637** (2022) .
- [6] R. Pilleri, E. Bissaldi, N. Omodei and F.L. G. La Mura, *Grb 221009a: Fermi-lat refined analysis*, *GCN Circ.* **32658** (2022) .
- [7] M. Axelsson, M. Ajello, M. Arimoto, L. Baldini, J. Ballet, M.G. Baring et al., *GRB 221009A: the B.O.A.T Burst that Shines in Gamma Rays*, *arXiv e-prints* (2024) arXiv:2409.04580 [2409.04580].
- [8] FERMI-LAT, FERMI-GBM collaboration, *GRB 221009A: the B.O.A.T Burst that Shines in Gamma Rays*, **2409.04580**.
- [9] K. Murase, M. Mukhopadhyay, A. Kheirandish, S.S. Kimura and K. Fang, *Neutrinos from the Brightest Gamma-Ray Burst?*, *Astrophys. J. Lett.* **941** (2022) L10 [2210.15625].
- [10] R. Alves Batista, *GRB 221009A: a potential source of ultra-high-energy cosmic rays*, *arXiv e-prints* (2022) arXiv:2210.12855 [2210.12855].
- [11] S. Das and S. Razzaque, *Ultrahigh-energy cosmic-ray signature in GRB 221009A*, *Astron. Astrophys.* **670** (2023) L12 [2210.13349].
- [12] N. Mirabal, *Secondary GeV-TeV emission from ultra-high-energy cosmic rays accelerated by GRB 221009A*, *Mon. Not. R. Astron. Soc.* **519** (2023) L85 [2210.14243].
- [13] K. Murase, *High-energy Emission Induced by Ultra-high-energy Photons as a Probe of Ultra-high-energy Cosmic-Ray Accelerators Embedded in the Cosmic Web*, *Astrophys. J. Lett.* **745** (2012) L16 [1111.0936].
- [14] H. Abdalla, S. Razzaque, M. Böttcher, J. Finke and A. Domínguez, *Influence of cosmic voids on the propagation of TeV gamma-rays and the puzzle of GRB 221009A*, *Mon. Not. R. Astron. Soc.* **532** (2024) 198 [2406.10651].
- [15] J.C. Joshi and S. Razzaque, *Modelling synchrotron and synchrotron self-Compton emission of gamma-ray burst afterglows from radio to very-high energies*, *Mon. Not. Roy. Astron. Soc.* **505** (2021) 1718 [1911.01558].
- [16] M. Barnard, S. Razzaque and J.C. Joshi, *Very high energy gamma-rays from GRB 180720B and GRB 190829A with external Compton emission*, *Mon. Not. R. Astron. Soc.* **527** (2024) 11893 [2312.14772].
- [17] J.D. Finke, S. Razzaque and C.D. Dermer, *Modeling the Extragalactic Background Light from Stars and Dust*, *Astrophys. J.* **712** (2010) 238 [0905.1115].
- [18] A. Domínguez, J.R. Primack, D.J. Rosario, F. Prada, R.C. Gilmore, S.M. Faber et al., *Extragalactic background light inferred from AEGIS galaxy-SED-type fractions*, *Mon. Not. R. Astron. Soc.* **410** (2011) 2556 [1007.1459].

- [19] H. Abdalla, R. Adam, F. Aharonian, F. Ait Benkhali, E.O. Angüner, M. Arakawa et al., *A very-high-energy component deep in the γ -ray burst afterglow*, *Nature* **575** (2019) 464.
- [20] MAGIC Collaboration, V.A. Acciari, S. Ansoldi, L.A. Antonelli, A. Arbet Engels, D. Baack et al., *Teraelectronvolt emission from the γ -ray burst GRB 190114C*, *Nature* **575** (2019) 455 [2006.07249].
- [21] H. Abdalla, F. Aharonian, F. Ait Benkhali, E.O. Angüner, C. Arcaro, C. Armand et al., *Revealing x-ray and gamma ray temporal and spectral similarities in the GRB 190829A afterglow*, *Science* **372** (2021) 1081.
- [22] E. Derishev and T. Piran, *The Physical Conditions of the Afterglow Implied by MAGIC's Sub-TeV Observations of GRB 190114C*, *Astrophys. J. Lett.* **880** (2019) L27 [1905.08285].
- [23] X.-Y. Wang, R.-Y. Liu, H.-M. Zhang, S.-Q. Xi and B. Zhang, *Synchrotron Self-Compton Emission from External Shocks as the Origin of the Sub-TeV Emission in GRB 180720B and GRB 190114C*, *Astrophys. J.* **884** (2019) 117 [1905.11312].
- [24] E. Derishev and T. Piran, *GRB Afterglow Parameters in the Era of TeV Observations: The Case of GRB 190114C*, *Astrophys. J.* **923** (2021) 135 [2106.12035].
- [25] Y. Sato, K. Obayashi, R. Yamazaki, K. Murase and Y. Ohira, *Off-axis jet scenario for early afterglow emission of low-luminosity gamma-ray burst GRB 190829A*, *Mon. Not. R. Astron. Soc.* **504** (2021) 5647 [2101.10581].
- [26] S. Yamasaki and T. Piran, *Analytic modelling of synchrotron self-Compton spectra: Application to GRB 190114C*, *Mon. Not. R. Astron. Soc.* **512** (2022) 2142 [2112.06945].
- [27] O.S. Salafia, M.E. Ravasio, J. Yang, T. An, M. Orienti, G. Ghirlanda et al., *Multiwavelength View of the Close-by GRB 190829A Sheds Light on Gamma-Ray Burst Physics*, *Astrophys. J. Lett.* **931** (2022) L19 [2106.07169].
- [28] Y. Sato, K. Obayashi, B.T. Zhang, S.J. Tanaka, K. Murase, Y. Ohira et al., *Synchrotron self-compton emission in the two-component jet model for gamma-ray bursts*, *JHEAp* **37** (2023) 51 [2208.13987].
- [29] B.T. Zhang, K. Murase, K. Ioka, D. Song, C. Yuan and P. Mészáros, *External Inverse-compton and Proton Synchrotron Emission from the Reverse Shock as the Origin of VHE Gamma Rays from the Hyper-bright GRB 221009A*, *Astrophys. J. Lett.* **947** (2023) L14 [2211.05754].
- [30] Y. Sato, K. Murase, Y. Ohira and R. Yamazaki, *Two-component jet model for multiwavelength afterglow emission of the extremely energetic burst GRB 221009A*, *Mon. Not. R. Astron. Soc.* **522** (2023) L56 [2212.09266].
- [31] J. Ren, Y. Wang and Z.-G. Dai, *Jet Structure and Burst Environment of GRB 221009A*, *Astrophys. J.* **962** (2024) 115 [2310.15886].
- [32] B.T. Zhang, K. Murase, K. Ioka and B. Zhang, *The origin of very-high-energy gamma-rays from GRB 221009A: Implications for reverse shock proton synchrotron emission*, *JHEAp* **45** (2025) 392 [2311.13671].
- [33] B. Banerjee, S. Macera, A. Ludovico De Santis, A. Mei, J. Tissino, G. Oganessian et al., *Camelidae on BOAT: observation of a second spectral component in GRB 221009A*, *arXiv e-prints* (2024) arXiv:2405.15855 [2405.15855].
- [34] Y. Sato, K. Murase, Y. Ohira, S. Inoue and R. Yamazaki, *Two-component jet model for the afterglow emission of GRB 201216C and GRB 221009A and implications for jet structure of very-high-energy gamma-ray bursts*, **2502.19051**.
- [35] E. Nakar, S. Ando and R. Sari, *Klein-Nishina effects on Synchrotron and Synchrotron self-Compton spectrum*, *Astrophys. J.* **703** (2009) 675 [0903.2557].

- [36] R. Sari, T. Piran and J.P. Halpern, *Jets in Gamma-Ray Bursts*, *Astrophys. J. Lett.* **519** (1999) L17 [[astro-ph/9903339](#)].
- [37] C.L. Carilli and G.B. Taylor, *Cluster Magnetic Fields*, *Annu. Rev. Astron. Astrophys.* **40** (2002) 319 [[astro-ph/0110655](#)].
- [38] K. Kotera and M. Lemoine, *The optical depth of the Universe for ultra-high energy cosmic ray scattering in the magnetized large scale structure*, *Phys. Rev. D* **77** (2008) 123003 [[0801.1450](#)].
- [39] C.D. Dermer, S. Razzaque, J.D. Finke and A. Atoyan, *Ultra-high-energy cosmic rays from black hole jets of radio galaxies*, *New Journal of Physics* **11** (2009) 065016 [[0811.1160](#)].
- [40] K. Murase, C.D. Dermer, H. Takami and G. Migliori, *Blazars as Ultra-High-Energy Cosmic-Ray Sources: Implications for TeV Gamma-Ray Observations*, *Astrophys. J.* **749** (2012) 63 [[1107.5576](#)].
- [41] H. Takami and K. Murase, *The Role of Structured Magnetic Fields on Constraining Properties of Transient Sources of Ultra-high-energy Cosmic Rays*, *Astrophys. J.* **748** (2012) 9 [[1110.3245](#)].
- [42] A. Neronov and I. Vovk, *Evidence for Strong Extragalactic Magnetic Fields from Fermi Observations of TeV Blazars*, *Science* **328** (2010) 73 [[1006.3504](#)].
- [43] F. Aharonian, J. Aschersleben, M. Backes, V.B. Martins, R. Batzofin, Y. Becherini et al., *Constraints on the Intergalactic Magnetic Field Using Fermi-LAT and H.E.S.S. Blazar Observations*, *Astrophys. J. Lett.* **950** (2023) L16 [[2306.05132](#)].
- [44] Z.G. Dai and T. Lu, *Spectrum and Duration of Delayed MeV-GeV Emission of Gamma-Ray Bursts in Cosmic Background Radiation Fields*, *Astrophys. J.* **580** (2002) 1013 [[astro-ph/0203084](#)].
- [45] S. Razzaque, P. Mészáros and B. Zhang, *GeV and Higher Energy Photon Interactions in Gamma-Ray Burst Fireballs and Surroundings*, *Astrophys. J.* **613** (2004) 1072 [[astro-ph/0404076](#)].
- [46] K. Murase, K. Asano and S. Nagataki, *Effects of Cosmic Infrared Background on High Energy Delayed Gamma-Rays from Gamma-Ray Bursts*, *Astrophys. J.* **671** (2007) 1886 [[astro-ph/0703759](#)].
- [47] K. Ichiki, S. Inoue and K. Takahashi, *Probing the Nature of the Weakest Intergalactic Magnetic Fields with the High-Energy Emission of Gamma-Ray Bursts*, *Astrophys. J.* **682** (2008) 127 [[0711.1589](#)].
- [48] K. Murase, K. Takahashi, S. Inoue, K. Ichiki and S. Nagataki, *Probing Intergalactic Magnetic Fields in the GLAST Era through Pair Echo Emission from TeV Blazars*, *Astrophys. J. Lett.* **686** (2008) L67 [[0806.2829](#)].
- [49] K. Murase, B. Zhang, K. Takahashi and S. Nagataki, *Possible effects of pair echoes on gamma-ray burst afterglow emission*, *Mon. Not. R. Astron. Soc.* **396** (2009) 1825 [[0812.0124](#)].
- [50] R. Alves Batista, A. Dundovic, M. Erdmann, K.-H. Kampert, D. Kuempel, G. Müller et al., *CRPropa 3 - a Public Astrophysical Simulation Framework for Propagating Extraterrestrial Ultra-High Energy Particles*, *JCAP* **05** (2016) 038 [[1603.07142](#)].
- [51] R. Alves Batista et al., *CRPropa 3.2 — an advanced framework for high-energy particle propagation in extragalactic and galactic spaces*, *JCAP* **09** (2022) 035 [[2208.00107](#)].
- [52] G.A. Medina-Tanco and T.A. Ensslin, *Isotropization of ultrahigh-energy cosmic ray arrival directions by radio ghosts*, *Astropart. Phys.* **16** (2001) 47 [[astro-ph/0011454](#)].
- [53] F. Marinacci et al., *First results from the IllustrisTNG simulations: radio haloes and magnetic fields*, *Mon. Not. Roy. Astron. Soc.* **480** (2018) 5113 [[1707.03396](#)].

- [54] S. Das, N. Gupta and S. Razzaque, *Ultrahigh-energy cosmic ray interactions as the origin of very high energy γ -rays from BL Lacs*, *Astrophys. J.* **889** (2020) 149 [[1911.06011](#)].
- [55] K. Murase, D. Guetta and M. Ahlers, *Hidden Cosmic-Ray Accelerators as an Origin of TeV-PeV Cosmic Neutrinos*, *Phys. Rev. Lett.* **116** (2016) 071101 [[1509.00805](#)].
- [56] O. Kalashev, A. Korochkin, A. Neronov and D. Semikoz, *Modeling the propagation of very-high-energy γ -rays with the CRbeam code: Comparison with CRPropa and ELMAG codes*, *Astron. Astrophys.* **675** (2023) A132 [[2201.03996](#)].
- [57] K. Murase, *Ultrahigh-Energy Photons as a Probe of Nearby Transient Ultrahigh-Energy Cosmic-Ray Sources and Possible Lorentz-Invariance Violation*, *Phys. Rev. Lett.* **103** (2009) 081102 [[0904.2087](#)].
- [58] E. Waxman and J.N. Bahcall, *Neutrino afterglow from gamma-ray bursts: Similar to 10^{18} -eV*, *Astrophys. J.* **541** (2000) 707 [[hep-ph/9909286](#)].
- [59] K. Murase, *High energy neutrino early afterglows gamma-ray bursts revisited*, *Phys. Rev. D* **76** (2007) 123001 [[0707.1140](#)].
- [60] S. Razzaque, *Long-lived PeV-EeV neutrinos from gamma-ray burst blastwave*, *Phys. Rev. D* **88** (2013) 103003 [[1307.7596](#)].
- [61] R. Plaga, *Detecting intergalactic magnetic fields using time delays in pulses of γ -rays*, *Nature* **374** (1995) 430.
- [62] K. Takahashi, K. Murase, K. Ichiki, S. Inoue and S. Nagataki, *Detectability of Pair Echoes from Gamma-Ray Bursts and Intergalactic Magnetic Fields*, *Astrophys. J. Lett.* **687** (2008) L5 [[0806.2825](#)].
- [63] I. Vovk, A. Korochkin, A. Neronov and D. Semikoz, *Constraints on the intergalactic magnetic field from Fermi/LAT observations of the ‘pair echo’ of GRB 221009A*, *Astron. Astrophys.* **683** (2024) A25.
- [64] R. Abbasi, M. Ackermann, J. Adams, S.K. Agarwalla, N. Aggarwal, J.A. Aguilar et al., *Limits on Neutrino Emission from GRB 221009A from MeV to PeV Using the IceCube Neutrino Observatory*, *Astrophys. J. Lett.* **946** (2023) L26 [[2302.05459](#)].
- [65] S. Aiello, A. Albert, M. Alshamsi, S. Alves Garre, A. Ambrosone, F. Ameli et al., *Search for neutrino emission from GRB 221009A using the KM3NeT ARCA and ORCA detectors*, *J. Cosmol. Astropart. Phys.* **2024** (2024) 006 [[2404.05354](#)].
- [66] K. Murase, M. Mukhopadhyay, A. Kheirandish, S.S. Kimura and K. Fang, *Neutrinos from the Brightest Gamma-Ray Burst?*, *Astrophys. J. Lett.* **941** (2022) L10 [[2210.15625](#)].
- [67] J.S. Bright et al., *Precise measurements of self-absorbed rising reverse shock emission from gamma-ray burst 221009A*, *Nature Astron.* **7** (2023) 986 [[2303.13583](#)].
- [68] R. Jia, W. Yun and D. Zi-Gao, *Jet Structure and Burst Environment of GRB 221009A*, *Astrophys. J.* **962** (2024) 115 [[2310.15886](#)].
- [69] B. O’Connor et al., *A structured jet explains the extreme GRB 221009A*, *Sci. Adv.* **9** (2023) adi1405 [[2302.07906](#)].
- [70] M. Negro et al., *The IXPE View of GRB 221009A*, *Astrophys. J. Lett.* **946** (2023) L21 [[2301.01798](#)].